Table 3 Cross-correlation coefficients among trace element compositions in *G. bulloides* and *G. inflata*, and palaeoclimatic indices in cores E49-19 and E48-22

E49-19

	Total fauna	% Sinistral *N. pachyderma*
Sr in *G. bulloides*	0.80*	−0.70*
Sr in *G. inflata*	0.77*	−0.69*
Mg in *G. bulloides*	0.64*	−0.51*
Mg in *G. inflata*	0.57*	−0.43*

E48-22

	Total fauna	% Sinistral *N. pachyderma*	$^{18}O/^{16}O$
Sr in *G. bulloides*	0.54*	−0.50*	−0.69*
Sr in *G. inflata*	0.19	−0.13	−0.38†
Mg in *G. bulloides*	0.43†	−0.36†	−0.44‡
Mg in *G. inflata*	0.30	−0.27	−0.29

These coefficients were determined for lags of zero, where correlations are normally at a maximum.
*$P \leq 0.001$; †$P \leq 0.05$; ‡$P \leq 0.01$.

differences exist over this narrow latitudinal belt (50–51°S), and differences in Mg should be due to dissolution. The Mg content does not change with water depth, and is also not related to the degree of fragmentation of the planktonic foraminiferal tests (Fig. 3). The degree of fragmentation has been shown[26,27] to represent a dissolution index in marine sediments. Therefore, it is less likely that the Mg signals in the cores are affected by dissolution. Likewise, no dissolution effects were found on Sr, which is in agreement with previous observations[28].

The results indicate that Sr concentrations in *G. bulloides* and *G. inflata* closely follow the late Quaternary climatic variations. The material available allowed only single analyses per sample; the precision of individual sample estimates could be improved by replicate analyses. Also, with further refinements of laboratory techniques, much of the 'noise' in the Sr curves might be reduced, which could aid in clarifying the palaeoclimatic signals. If so, Sr concentrations in these and other planktonic foraminiferal species, are a new independent means for palaeoclimatic analysis of Quaternary and, possibly, older sediments.

This research was supported by grant G4076-101 from the Swedish Natural Science Research Council. We thank Drs M. L. Bender, J. P. Kennett, F. T. Manheim and L. Sjöberg for helpful comments, and D. S. Cassidy for providing the material from the South Atlantic. Chemical analyses were made by Adnan Fahmy, Stockholm University.

Received 6 October 1980; accepted 23 February 1981.

1. Clarke, F. W. & Wheeler, W. C. *U.S. geol. Surv. Prof. Pap.* **124,** 1–62 (1922).
2. Chave, K. E. *J. Geol.* **62,** 266–283 (1954).
3. Chave, K. E. *J. Geol.* **62,** 587–599 (1954).
4. Blackmon, P. D. & Todd, R. *J. Paleont.* **33,** 1–15 (1959).
5. Dodd, J. R. *Geochim. cosmochim. Acta* **29,** 385–398 (1965).
6. Schopf, T. J. M. & Manheim, F. T. *J. Paleont.* **41,** 1197–1225 (1967).
7. Zolotarev, V. N. *Geochem. Int.* **11,** 347–352 (1975).
8. Krinsley, D. *Micropaleontology* **6,** 297–300 (1960).
9. Savin, S. M. & Douglas, R. G. *Bull. Geol. Soc. Am.* **84,** 2327–2342 (1973).
10. Bender, M. L., Lorens, R. B. & Williams, D. F. *Micropaleontology* **21,** 448–459 (1975).
11. Ragland, P. C., Pilkey, O. H. & Blackwelder, B. W. *Chem. Geol.* **25,** 123–134 (1979).
12. Windom, H. L. & Smith, R. G. *Southeastern Geol.* **13,** 275–281 (1971).
13. Bé, A. W. H. in *Oceanic Micropaleontology* Vol. 1 (ed. Ramsay, A. T. S.) 1–100 (Academic, London, 1977).
14. Emiliani, C. *Science* **173,** 1122–1124 (1971).
15. Berger, W. H., Killingley, J. S. & Vincent, E. *Oceanol. Acta* **1,** 203–216 (1978).
16. Williams, D. F. *Mar. Micropaleont.* **1,** 363–375 (1976).
17. Malmgren, B. A. & Kennett, J. P. *J. Paleont.* **52,** 1195–1207 (1978).
18. Towe, K. M. & Lowenstam, H. A. *J. ultrastruct. Res.* **17,** 1–13 (1967).
19. Travis, D. F. *Ann. N.Y. Acad. Sci.* **109,** 177–245 (1963).
20. Harrison, P. M. in *Iron Metabolism—An International Symposium*, 40–56 (Springer, Berlin, 1964).
21. Reimann, B. E. F. *Cell. Res.* **34,** 605–608 (1965).
22. Krauskopf, K. *Introduction to Geochemistry* (McGraw-Hill, New York, 1967).
23. Curtis, C. D. & Krinsley, D. *Geochim. cosmochim. Acta* **29,** 71–84 (1965).
24. Kilbourne, R. T. & Sen Gupta, B. K. *Geol. Soc. Am., Southeastern Sect., 22nd A. Meet. (Abstr.)* **5,** 408–409 (1973).
25. Jørgensen, N. O. *Bull. geol. Soc. Denmark* **24,** 299–325 (1975).
26. Thiede, J. *Bull. geol. Soc. Am.* **84,** 2749–2754 (1973).
27. Thunell, R. C. *Quat. Res.* **6,** 281–297 (1976).
28. Lorens, R. B., Williams, D. F. & Bender, M. L. *J. sedm. Petrol.* **47,** 1602–1609 (1977).

Intra-sex and inter-sex sibling interactions as sex ratio determinants

P. D. Taylor

Department of Mathematics and Statistics, Queen's University, Kingston, Ontario, Canada K7L 3N6

Fisher[1] produced the first general argument that a random-mating sexually-reproducing population should devote equal reproductive resources to the production of male and female offspring, while Hamilton[2] considered several unusual situations in which the expenditure of reproductive resources should be biased towards one sex or the other. His 'host' model has been widely cited[3–6] and at least three factors proposed as the cause of the sex ratio bias: local mate competition, sib-mating and inbreeding. The problem of which of these factors is the real cause of the biased sex ratio seems important in view of the large number of apparently different but often closely related sex ratio models which are now being proposed. It would be useful to have ways of classifying them according to the presence of different factors which affect the equilibrium sex ratio. Here, I present a general equation (equation (2)) for differential change in fitness which exhibits the equilibrium sex ratio as achieving a balance between the factor contained in Fisher's standard grandchild argument[1] and a second factor resulting from intra-sex sibling interactions over reproductive resources. In particular, I analyse Hamilton's host model[2] for the presence of these different factors.

I will present the model for the special case of discrete non-overlapping generations. Although many of the phenomena I wish to study lie outside this special case, the formulation of the model is complicated by the mixing of generations, and it seems best to start with a simple situation. We divide the life cycle of the organism into two phases. Phase 1 encompasses the time from birth to the point at which some significant sex-specific behaviour begins, and phase 2 continues from there to the birth of the next generation. The purpose of the model is to relate the effects of sex-specific sib interactions in phase 2 to the equilibrium sex ratio.

Suppose in the population a typical mated female produces a total of x^* daughters and y^* sons at the end of phase 1. Consider a rare female who manages to produce x daughters and y sons. Her fitness in the *-population will be

$$w(x, y) = D(x, y)x + S(x, y)y \quad (1)$$

where D is her expected ultimate genetic contribution through daughters per daughter and S is her expected contribution through sons per son. If at the end of phase 1, the offspring disperse at random into the general population, with no further non random sib interaction, then $D(x, y)$ and $S(x, y)$ are constants equal to their values D^* and S^* at (x^*, y^*); but otherwise they may not be constant.

Constraints operating during phase 1 will restrict the possible values of x and y in the population to a one-parameter family parameterized by the proportion r of reproductive resources allocated by the mother to the production of sons. In the simple case of a linear interchange between sons and daughters, with both sexes equally expensive, we have $x = K(1-r)$ and $y = Kr$, where K is the litter size. With this parameterization, w, D and S become functions of r and the value of dw/dr at $r = r^*$ (the value giving x^* and y^*) is a measure of the evolutionary pressure for an increase in r^*. If $dw/dr > 0$ we expect the population to evolve towards an increase in the proportion of resources allocated to the production of sons; if $dw/dr < 0$, this proportion should decrease. Now, differentiating equation (1),

0028-0836/81/190064—03$01.00

$$\frac{dw}{dr}=\left[D^*\frac{dx}{dr}+S^*\frac{dy}{dr}\right]$$

$$+\left[\frac{\partial D}{\partial x}\frac{dx}{dr}+\frac{\partial D}{\partial y}\frac{dy}{dr}+\frac{\partial S}{\partial x}\frac{dx}{dr}+\frac{\partial S}{\partial y}\frac{dy}{dr}\right] \quad (2)$$

where everything is evaluated at r^*. The second term on the right measures the effect of sibling interactions in phase 2 on the mother's reproductive success, and it vanishes in the absence of these. Let us interpret the four summands of this term.

The partial derivative $\partial D/\partial x$ measures the change in the quantity 'fitness through daughters per daughter' per extra daughter, with number of sons, y, held constant. Thus, it measures the influence of extra daughters on the reproductive success of each daughter. For example, competition among daughters for reproductive resources during phase 2 would tend to make $\partial D/\partial x<0$. Similarly, the analogous term $\partial S/\partial y$ measures absence of competition among brothers for reproductive resources. The cross term $\partial D/\partial y$ measures the influence of extra sons on the reproductive success of each daughter and similarly $\partial S/\partial x$ measures the influence of extra daughters on the reproductive success of each son.

Let us consider some examples. Clark[7] has studied African galagos in which young males disperse, but females remain within their home ranges and compete with their mother and sisters for reproductive resources (space, food). The resulting competition between sisters may contribute negatively to $\partial D/\partial x$. In MacDonald's foxes[8], females form cooperative breeding groups in which non-breeding vixens seem to confer benefits on the mother. There is strong evidence that members of a group are closely related, contributing positively to $\partial D/\partial x$.

Where males enhance the reproductive success of their sisters, we may get a positive contribution to $\partial D/\partial y$. Woolfenden[9] has shown that male helpers at the Florida scrub jay nest can have a significant effect on reproductive output. In all three of the above examples much of the interaction is between generations and may have important effects on the equilibrium sex ratio. However, the simple assumption of our model of non-overlapping generations restricts our attention to interaction within the same generation.

If competition between males for mates is more intense between brothers than between unrelated males, this contributes negatively to $\partial S/\partial y$. Partial sib-mating often has this effect, because brothers are competing for their sisters. Positive contributions to $\partial S/\partial y$ may result from cooperative behaviour among brothers. This is apparently the case, for example, for the lions studied by Bertram[10], who often hunt together and protect one another.

Partial sib mating also contributes positively to $\partial S/\partial x$, since extra daughters will increase the reproductive success of the sons. It is not so easy to find other examples in which daughters affect the reproductive success of their brothers. Pickering[11] describes a parasitoid wasp in which larval sibs growing on the host pupa compete for food. There is evidence that female larvae behave less altruistically towards their brothers than their sisters. An extra sister will affect both male and female reproductive success, but the effect on males may be greater.

To make specific calculations, we must find expressions for D and S in terms of x, y, x^* and y^*. In the above example of Pickering, the organisms are haplodiploid, and the resulting genetic asymmetry between males and females makes it difficult to find comparable measures for D and S. In this case special arguments are required[6,12]. The calculation of equilibrium sex ratio is further complicated by a conflict between mother and daughter over sex ratio[3,13]. In our calculations I will assume a diploid population. In this case, D and S can be calculated using the common measure of mated females; each mated daughter counts 1 and each female mated exclusively by a son counts 1 (with shared matings discounted by the appropriate factor). From this method of counting it follows that $D^*x^*=S^*y^*$.

The equilibrium value of r^* is obtained by setting dw/dr, given by equation (2), equal to zero. An examination of the various terms of equation (2) at equilibrium will display the different forces (on the value of r^*) which are held in balance at equilibrium.

As a normative example, consider Fisher's standard situation[1] in which offspring disperse after phase 1 and mate at random. Then $D(x,y)=D^*$, $S(x,y)=S^*=D^*x^*/y^*$, $x=K(1-r)$ and $y=Kr$. Therefore, all partial derivatives of D and S vanish, and equation (2) becomes

$$-D^*K+D^*K(1-r^*)/r^*$$

which, when set equal to zero, gives the equilibrium value $r^*=\frac{1}{2}$. We will refer to the first bracket in equation (2) as the Fisher term, as this is the term which must vanish at equilibrium in his standard model.

In Hamilton's model[2], mated females collect on hosts in random groups of size N to produce and raise K offspring each. At the start of phase 2, the KN offspring mate at random among themselves, and the mated females go out into the general population to form new host groups and start the cycle again. Because a mutant female is rare we can assume the other females in her host group are normal. Hence, $D(x,y)=D^*$ and $S(x,y)=D^*(x+(N-1)x^*)/(y+(N-1)y^*)$. With these expressions both partial derivatives of D vanish, $\partial S/\partial x$ is positive because of the sib-mating and $\partial S/\partial y$ is negative because of male reproductive competition resulting from the sib-mating. Then equation (2) has the form

$$D^*\left[\frac{dx}{dr}+\frac{x^*}{y^*}\frac{dy}{dr}\right]+\left[\frac{\partial S}{\partial x}\frac{dx}{dr}+\frac{\partial S}{\partial y}\frac{dy}{dr}\right]$$

Since $dx/dr<0$ and $dy/dr>0$ both terms in the second bracket are negative, and both act in the same way on r^*. At equilibrium the Fisher term must be positive, requiring a female-biased sex-ratio. With $x=K(1-r)$ and $y=Kr$, the equilibrium ratio turns out to be $r^*=(N-1)/2N$. Thus, the female bias, which is often loosely thought to result from sib-mating, actually results from two different forces: the effect of extra daughters on male mating success, and the effect of fewer sons on male reproductive competition.

Finally, the general model applies equally well to the model of Charnov[14] for barnacles and Fischer[15] for coral reef fish, of sex allocation in hermaphrodites. (Replace mated female by individual, daughter and son by egg and sperm, and the process of mating by that of fertilization.) Each individual delivers its sperm to fertilize the eggs of N other individuals, and has its own eggs fertilized by, on average, N other individuals. As before a linear tradeoff is assumed between production of eggs x and sperm y. Thus $D(x,y)=D^*$ and $S(x,y)=D^*Nx^*/(y+(N-1)y^*)$. This is formally the same as Hamiltonian's model, except that we have removed the possibility of sib-mating, and $\partial S/\partial x$ is now zero. However, $\partial S/\partial y$ is the same as before, again forcing the Fisher term to be positive, creating a female-biased equilibrium ratio, this time, only through the effect of fewer sons on male reproductive competition.

The significance of equation (2) is that it resolves the evolutionary pressure on r^* into a sum of two factors which are held in balance at equilibrium: the standard Fisher factor and a second factor containing the effect of intra- and inter-sex sibling interactions. This second factor again resolves into four terms. Different sex ratio models can be compared according to the presence of these factors. Sib-mating (or selfing in hermaphrodites) or more generally mating between relatives, often contributes to these factors, but the inbreeding which results, in itself, has no role in determining sex ratio.

This research was supported by a grant from the Natural Sciences and Engineering Research Council of Canada. I thank Michael Bulmer for many discussions which sharpened my understanding of the causes of sex ratio bias and George Williams for valuable comments on the first draft.

Received 18 August 1980; accepted 26 February 1981.

1. Fisher, R. A. *The Genetical Theory of Natural Selection* (Oxford University Press, 1929).
2. Hamilton, W. D. *Science* **156,** 477–488 (1967).
3. Trivers, R. L. & Hare, H. *Science* **191,** 249–263 (1976).
4. Stenseth, N. C. *Oikos* **30,** 83–89 (1978).
5. Maynard Smith, J. *The Evolution of Sex* (Cambridge University Press, 1978).
6. Taylor, P. D. & Bulmer, M. G. *J. theor. Biol.* **86,** 409–419 (1980).
7. Clark, A. B. *Science* **201,** 163–165 (1978).
8. MacDonald, D. W. *Nature* **282,** 69–71 (1979).
9. Emlen, S. T. in *Behavioural Ecology* (eds Krebs, J. R. & Davies, N. B.) 245–281 (Blackwell, Oxford, 1978).
10. Bertram, B. C. R. in *Behavioural Ecology* (eds Krebs, J. R. & Davies, N. B.) 64–96 (Blackwell, Oxford 1978).
11. Pickering, J. *Nature* **283,** 291–292 (1980).
12. Benford, F. A. *J. theor. Biol.* **72,** 701–727 (1978).
13. Bulmer, M. G. & Taylor, P. D. *Heredity* (in the press).
14. Charnov, E. L. *Mar. Biol. Lett.* **1,** 269–272 (1980).
15. Fischer, E. A. *Am. Nat.* **17,** 64–82 (1981).

Retinal projection in a non-visual area after bilateral tectal ablation in goldfish

S. C. Sharma

Department of Ophthalmology, New York Medical College, Valhalla, New York 10595, USA

If, in the adult goldfish, one optic tectum is ablated, the regenerating optic axons from the contralateral retina innervate the remaining tectum, where they form a retinotopically ordered map[1–3]. The pathway for this induced ipsilateral projection[1] coincides with many of the pathways which normally connect the two tecta, but early in regeneration the optic fibres also enter non-visual centres to which there are degenerating tectal efferent pathways to follow[4]. We have therefore now investigated the fate of regenerating optic axons in goldfish from which both optic tecta have been removed; they are found to innervate non-visual centres, where again they generate a retinotopic map.

Fifteen adult goldfish (10–12 cm long and 2.5 yr old at the time of surgery) were anaesthetized with 0.5% MS222. The tectum was ablated bilaterally and extreme care taken not to damage the diencephalon, which joins the tectum at its rostral pole. Animals were allowed to survive between 380 and 620 days after tectal removal before electrophysiological mappings of the retinal projections were made. In five animals, the right eye was injected with 10 μl of [3,4-^{3}H]proline (specific activity 50 Ci mmol^{-1}) 1 day before mapping; the brains of these animals were processed for autoradiography. In five other animals, after visuotopic mapping, the right optic nerve was cut and 50% horseradish peroxidase (HRP) solution (Sigma type VI) applied to the cut end. The retinal projection of the remaining five animals was studied anatomically, using HRP orthograde transportation after injection of 5–7 μl of 30% HRP intraocularly. In the HRP studies, animals were killed 1–3 days later and processed for HRP reaction[5].

Autoradiographic analysis showed that, in addition to a high concentration of termination sites in the primary diencephalic visual centres, the optic fibres terminated in most tectal efferent areas[6,7]. In normal fish these areas do not receive direct retinal fibre terminations[8,9] and include the tori semicircularis, nucleus isthmi, nucleus of the rostral mesencephalic tegmentum, dorsolateral tegmental nucleus and nucleus reticularis superior of the hindbrain. In addition, radioactive grains were seen in the rostral valvula cerebelli.

Orthograde transport of HRP studied in 10 animals basically confirmed the autoradiographic identification of target centres of regenerating optic axons (Fig. 1). Most optic fibre fascicles in the regenerated optic nerve appear linearly arranged. The optic fibre fascicles separate from the ventral part of the optic tract at the diencephalic level and travel caudally before arborizing. The first bundle of optic fibres detached itself from the nerve at its rostral ventral position then the next dorsal bundle did the same. The uppermost portion of the nerve travelled farthest and apparently terminated in the valvula cerebelli (Fig. 1*b*, *c*). This pattern of axonal trajectories from the optic nerve is similar to that observed in normal goldfish (S.C.S., unpublished observation).

The visuotopic projection of either the right or left eye was determined in 10 animals by electrophysiologically mapping the area directly beneath the ablated tectum. This area includes the valvula cerebelli medially and the torus semicircularis laterally and ventrally. The visuotopic projection represented in Fig. 2 was essentially similar to that seen in eight other animals and was confined to the rostro-medial portion of the contralateral valvula cerebelli. The projection map in the remaining animal was incomplete. The representation of the superior contralateral visual field was similar in its extent to a normal visuotopic projection onto the contralateral tectum. The receptive field sizes of the multi-units were in the 10–15° range, which is similar to the size of normal retinotectal units.

In three animals, in addition to the projection to the valvula cerebelli, large receptive fields (60–80°) were recorded from the torus semicircularis and were mostly from the inferior visual field. It was not possible to record any meaningful visuotopic maps from the torus. Large receptive field units were also recorded from the the deeper tegmental areas.

These results imply that, in the absence of both optic tecta, the optic axons can regenerate to non-visual centres and generate a retinotopic projection which approximates to the normal map. As the retinotopic map represents presynaptic optic fibre terminations, it is not certain whether fibres formed synaptic connections with cells in anomalous areas. Anomalous connections to non-visual targets following one tectal removal have been reported in various vertebrates[10–13].

The valvula cerebelli extend rostrally into the optic ventricle and lie apposed to the ventral surface of the dorsal tectum

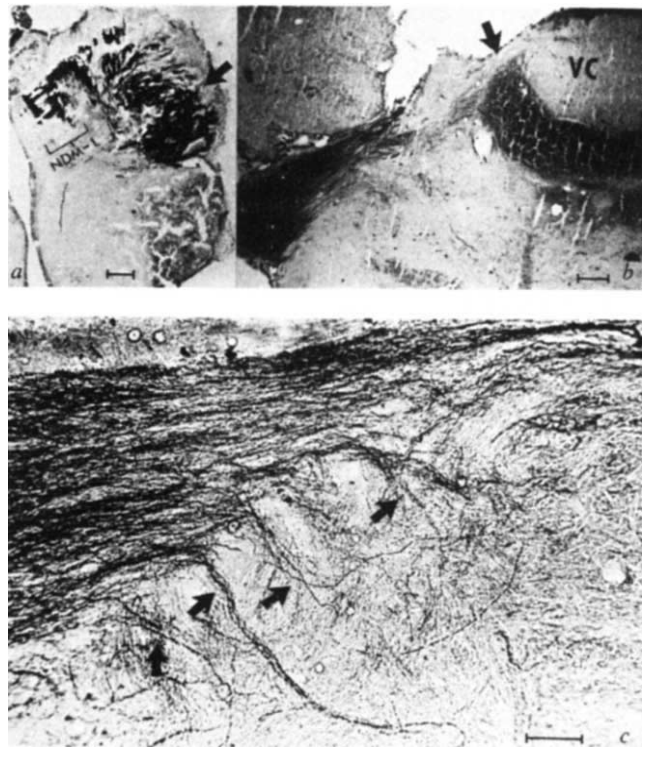

Fig. 1 *a*, Coronal section through the diencephalon showing contralateral retinal projection in a fish 380 days after tectal ablation where the eye was injected with HRP. The medial diencephalic retinal target areas (nucleus dorsalis medialis and lateralis, NDM, NDL are heavily labelled. The arrow points to a neuroma (a misleading entity as neuroma does not appear in sagittally sectioned brains). Scale bar, 100 μm. *b*, Sagittal section through the brain of a fish 390 days after tectal ablation. The arrow points to the fibre entering the valvula cerebelli (VC). Scale bar, 100 μm. *c*, High power photomicrograph of the optic nerve from *b*. The arrows point to optic fascicles separating from the nerve. Scale bar, 100 μm.

0028–0836/81/190066—02$01.00